

HYDRODYNAMIC ANALYSIS OF GRAVITY NET CAGE IN OPEN SEA

Pedro V. H. V. Garcia, Artur F. Lagemann, Paulo F. Lamarão, Walter J. P. Casas

*Department of Mechanical Engineering, Federal University of Rio Grande do Sul
Rua Sarmiento Leite 435, 90050-170, Porto Alegre/Rio Grande do Sul, Brasil
pedrovictor86@gmail.com, arturlagemann@gmail.com,
paulo.fiuza.lamarao@gmail.com, walter.paucar.casas@ufrgs.br*

Abstract. This work is orientated towards modeling the hydrodynamic response of a circular net cage for fish-farming, submitted to the wave conditions of the city of Rio Grande - Rio Grande do Sul (RS). For this purpose, several routines were created using the MATLAB program, in order to determine the hydrostatic equilibrium of the structure, the drag force acting on the cage's net and the mooring systems using different materials. In possession of given data and taking into account the wave regimes of the study site, simulations were performed using the ANSYS AQWA software in order to obtain the cable tensions and the net cage behavior. Thereby, it can be noted that the break strength of the mooring system cables was not exceeded and the mooring systems were effective to keep the structure stable. At last, the modeling of the drag force acting on the net with the software used, by applying the drag coefficient formula, proved to be an acceptable solution for questions involving net cage. However, it is important to emphasize that the model used does not consider the non-linearity of the net. Also, the study suggests the installation of a smaller diameter net cage for pisciculture at the study site.

Keywords: Net cage, Hydrodynamic simulation, Catenary, Wave, Drag force.

1 Introduction

The increasing demand of fish into global market (FAO [1]) associated with an increase in the percentage of coastal areas occupation, studies on offshore pisciculture becomes more necessary. Within this scope, research involving the usage of floating net cages for fish-farming has become more common, as well as the factors related to its application.

One of these factors is the drag force acting on the cage's nets. Lader and Enerhaug [2] verified that the drag coefficient can be determined by the geometry of the net. Additionally, Dong *et al.* [3] showed that the vertical length of the net is the variable that most influences the drag coefficient. Another important factor is the mooring system of the structure. Júnior [4] makes use of an mooring system called "Pata de Galo". In addition, Assis [5] recommends that the minimum horizontal distance from the anchor to the structure should be three times greater than the depth of the seabed at the chosen site and presents the most used materials for the construction of a conventional mooring system. Finally, the analysis of the stability of the structure is a relevant factor. According to research by Dong *et al.* [3], the weight of the base of the cage has the greatest contribution for stability. From Kim *et al.* [6], tension in the anchor line is a critical factor for stability.

Taking those papers into account, it is necessary to carry out a hydrodynamic simulation that considers the drag force and the mooring system to analyze the response of the structure under regular waves. Furthermore, it is important to assess the stability of the net cage when it is exposed to specific sea conditions.

2 Modeling

For the hydrodynamic simulation performed in Ansys AQWA, monochromatic waves, based on the sea state at the region of Rio Grande, were used. Defining that all waves that will be simulated belong to the Airy wave regime, the term of speed (U) can be described according to the eq. (1) and (2) (Dean and Dalrymple [7]):

$$U_x(x, z, t) = \frac{H\sigma \cosh(k(h+z))}{2 \sinh(kh)} \cos(kx - \sigma t) = U_x(z) \cos(kx - \sigma t), \quad (1)$$

$$U_z(x, z, t) = \frac{H\sigma \sinh(k(h+z))}{2 \sinh(kh)} \cos(kx - \sigma t) = U_z(z) \sin(kx - \sigma t). \quad (2)$$

In this case H is the wave height, σ the angular frequency, k the wave number, h the depth, t the time, x the horizontal position and z the vertical position. Analyzing the eq. 1, the speed is composed by two parts, one is a function of the vertical position $U_x(z)$ and the other a function of the horizontal position and time. The pressure during the passage of a wave is given by eq. (3), where the first portion refers to the hydrostatic pressure and the second one to the dynamic pressure (P_d):

$$P(x, z, t) = -\rho g z + \rho g H \frac{\cosh(k(h+z))}{2 \cosh(kh)} \cos(kx - \sigma t). \quad (3)$$

$P_{(x,z,t)}$ is the total pressure, ρ the water density and g the gravitational acceleration. As one of the main loads in the structure caused by the drag force acting on the structure's net, the incorporation of this force F_{drag} is done according to the eq. (4) in which C_d is the drag coefficient and A_r the cross-sectional area perpendicular to the fluid flow, (Faltinsen [8]):

$$F_{drag} = \frac{1}{2} \rho C_d A_r U^2. \quad (4)$$

In order to obtain the drag force, eq. (4), the value of the drag coefficient is required, which is obtained experimentally. Based on Lader and Enerhaug [2] experiments, the equation that better estimates the drag coefficient for a net is:

$$C_{d_n} = 0.04 + (-0.04 + 0.33SL + 6.54SL^2 - 4.88SL^3) \cos(\alpha). \quad (5)$$

In this case α is the angle between the horizontal vector of the water particle speed and the normal direction of the net. Furthermore, SL denotes the net's solidity, defined by the projected area of the twines divided on the total circumscribed area of the net (Lader and Enerhaug [2]), which is equal to 0.225 in this paper. In order to define C_{d_n} a iterative routine, varying the alpha angle, was elaborated using MATLAB, responsible for solving the eq. (5) and (6):

$$\sum M = M_{F_{drag}} - M_{P_{ring}} = 0, \quad (6)$$

in which P_{ring} is the weight of the bottom ring and $M_{P_{ring}}$ is the momentum of it in relation to the upper ring and $M_{F_{drag}}$ is the momentum of the F_{drag} in relation to the upper ring (Fig. 1). The C_{d_n} routine returned the value equal to 0.3495.

For the next step, a routine for the catenary sizing was elaborated using MATLAB based on the local depth, all forces caused by the structure and a vector of W_{water} (weight per meter of the cable in the water). The following variables are obtained: the total cable length (l), the suspended cable length (l_r), the horizontal projection of the structure in the reference position (FP), the length of the cable on the seabed (L), the force on the cable (F), the horizontal component of F (F_x), the angle (θ) between the water line and the cable and the variation of the horizontal position of the net cage (ν) (Faltinsen [8]). Analyzing the catenary in the reference position ($\nu = 0$) and in the displaced position ($l_r = l$), we have the corresponding sub-indexes (1 and 2) in Fig. 2.

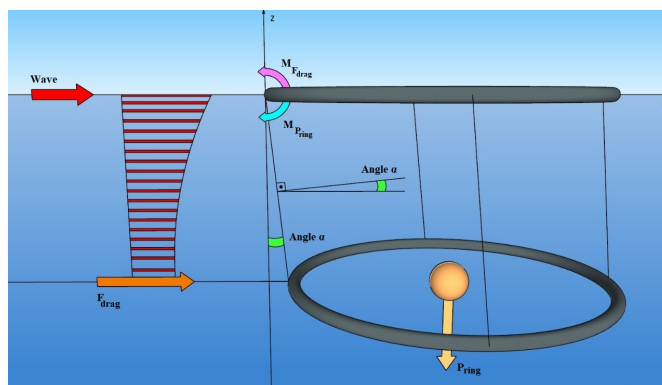


Figure 1. Sketch for drag evaluation

$$l_r = \frac{F}{W_{water}} \sinh\left(\frac{W_{water}}{F} x\right) \tag{7}$$

In addition to this, is added a database containing the mass per meter of the material in air (w_{air}) and the break strength of the material (BS) properties for different construction materials. Such data were taken from BRIDON [9] and Wichers [10]. Keeping with the Assis [5] convention, those cables that provided the greatest total length were chosen. The selected catenaries and materials for the simulation are shown in Table 1.

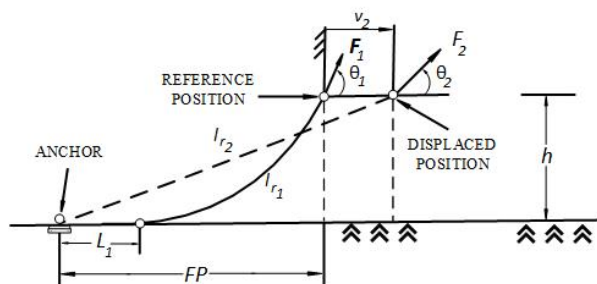


Figure 2. Illustration of a catenary and its parameters based on Wilson [11]

Table 1. Selected catenaries and materials properties for the simulation

Catenary	Material	l_1 [m]	l_{r1} [m]	w_{air} [kg/m]	FP [m]	θ_1 [°]	ν_2 [m]	F_1/BS [%]
1	Chain	65.70	39.39	9.20	62.77	36.53	1.20	3.43
2	Steel cable 1	45.42	28.29	21.00	41.25	49.36	1.65	0.37
3	Steel cable 2	55.39	33.70	12.60	51.94	42.19	1.39	0.59
4	Polyester	115.21	67.36	10.00	113.52	21.85	0.70	0.33

Afterwards, the dimensions of the net cage and the geometry of the mooring system were based on Júnior [4]. The mooring system consists of 4 buoys, each stabilized by 2 catenaries and dimensioned in hydrostatic condition, in order to withstand the heaviest catenaries. In addition, linear cables of stiffness equal to 100,000 [N/m] are used, considered undeformed for the situation, connecting the upper ring with the lower ring, the buoys between themselves and the buoys with the upper ring as shown in the Fig. 3.

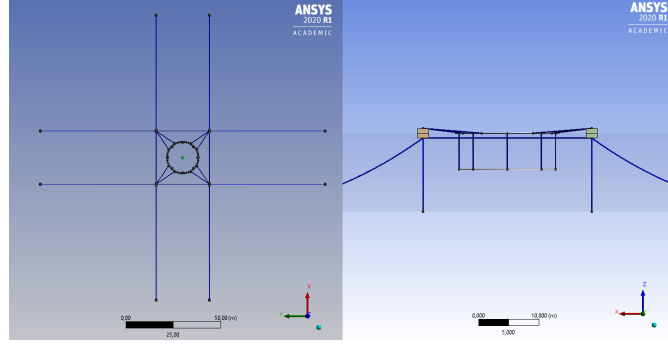


Figure 3. Mooring system configuration - "Pata de Galo"

In the initial condition, the positioning of the upper and lower rings in the water column was calculated using hydrostatic equilibrium equation:

$$F_w - B = F_w - g\rho \cdot (2\pi R \cdot A_{h_s}), \quad (8)$$

$$A_{h_s} = \frac{(\pi \cdot r^2)}{2} - r^2 \sin^{-1}\left(\frac{r - h_s}{r}\right) + (h_s - r) \sqrt{r^2 - (h_s - r)^2}. \quad (9)$$

The buoyancy generated is a function of the section area (A_{h_s}) and the submerged height (h_s), measured from the base of the ring's section to the submerged section eq. (9). The other variables are: F_w being the weight force, B the buoyancy, R the average radius of the rings (8 m) and r the radius of the ring's section (0.125 m).

The hydrodynamic behavior for each net cage's ring is modeled based on a mass-spring-damper system, described by the eq. (10), (Chakrabarti [12]):

$$M_T \ddot{x}(t) + C \dot{x}(t) + K x(t) = F_{ext}(t), \quad (10)$$

where the 6x6 matrices M_T , C and K are defined respectively as: the sum of structural and additional mass, the viscous damping and the stiffness of the cable added to the structural stiffness portion. The 6x1 vectors \ddot{x} , \dot{x} and x represent acceleration, velocity and displacement in the three translations directions and three rotations axis.

The excitation forces are represented by the vector $F_{ext}(t)$, which, considering the dimensions of the structure in relation to the wavelength, are described by the equation:

$$F_{ext}(t) = F_{FK}(t) + F_M + F_{drag} + F_{anc}, \quad (11)$$

in which $F_{FK}(t)$ corresponds to Froude-Krylov's force, F_M to Morison's force on the structure, F_{drag} to the drag force on the cage's net and F_{anc} to the force due to catenary cable.

Froude-Krylov's force is induced on the structure by the pressure field generated by waves not disturbed due to the structure presence. According to Chakrabarti [12], it is represented by the integral of the dynamic pressure along the submerged surface given by the equation:

$$F_{FK_x} = C_H \int \int_S P_d n_x dS. \quad (12)$$

C_H is a force coefficient related to the horizontal portion, n_x is the normal direction of the horizontal axes and S represents the body's surface. Likewise, the vertical component of Froude-Krylov's force is determined, with a vertical force coefficient C_V and direction z .

The Morison force is described by eq. (13), where C_m is the inertia coefficient, V the submerged volume, $\frac{du_i}{dt}$ the theoretical acceleration of the water particle, A_a the area perpendicular to the flow and i the component (x, y, z) directions:

$$F_{m_i} = \rho C_m V \frac{du_i}{dt} + \frac{1}{2} \rho C_d A_a |u_i| u_i. \quad (13)$$

To solve these equations, the Ansys AQWA software hydrodynamic diffraction toolbox divides the structure into discrete parts, using the panel method, to calculate the potential flow around the body. Afterwards, it applies the boundary conditions necessary to solve the differential equations.

In sequence, the mesh validation process was carried out according to Massie [13], running several simulations with an increment in the number of panels until the convergence of the analytical mass and calculated mass into the equilibrium condition. Thus, a mesh with an error of up to 5% was chosen. For the time-step, the Ansys manual [14] suggests a maximum period of 1/10 of the wave period. Starting from the period 0.45 s and decreasing progressively until convergence, the selected period was 0.01 s.

3 Simulations

At the simulation step, the four catenaries (from Table 1) were simulated using parametric variations of waves according to Table 2. These simulations were defined for the average height and periods chosen as equally spaced around the average period, based on the oceanographic data of the Brazilian coast monitoring system (SiMCosta [15]), from 02/19/2019 to 04/23/2020, provided by an acquisition buoy at a depth of 13 m, located at the Cassino beach, in the city of Rio Grande-RS.

Table 2. Simulated waves

Wave	Height [m]	Period [s]
1	0.72	4.5
2	0.72	5.0
3	0.72	5.5
4	0.72	6.0

4 Results

Different waves excitation for each catenary were plotted in graphs and analyzed. Therewith, it was possible to calculate the ratio between the maximum theoretical force to move the anchor (F_2) and the maximum force returned by the simulation, that are displayed in Table 3. From that, for values under 1 the anchor is moved, for values greater than 1 the condition is safe. According to the ratio, catenary 1 proved to be insufficient for the application, were as catenaries 3 and 4 are safer. Regarding to the break strength of the catenaries materials, the maximum tension found in the simulations was less than 5% of it. With respect to the other cable ones, the simulations showed low tension values.

Table 3. Catenary ratios

Wave	Catenary 1	Catenary 2	Catenary 3	Catenary 4
1	1.59	1.69	1.98	2.12
2	1.49	1.57	1.69	1.71
3	1.50	1.70	1.94	2.08
4	0.69	1.27	1.73	1.89

Analyzing the response graphs in relation to the z position of the upper ring (Fig.4), which is modeled as a rigid body in the software, it can be observed that when the structure's center is located in the wave's trough the ring is supported by two points, both adjacent wave crests. When the structure's center is at the wave's crest, that

point is the only supported. However, even for the shortest period of the wave, the structure has a maximum water column pressure of approximately 0.2 m. In the static condition, it would probably be within the elastic regime of a 16 m beam model (diameter of the circular net cage). Even so, as the loads are dynamic, the structure could suffer damages related to fatigue.

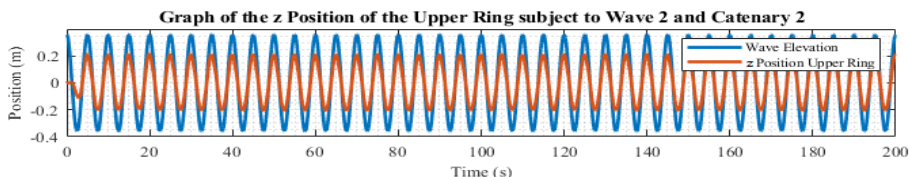


Figure 4. Comparison between wave 2 elevation and the Z position of the upper ring, considering catenary 2

The result of the X position of the lower ring (Fig.5) is out of phase with the upper ring and consequently with the wave elevation. This result indicates inertial characteristics of the analyzed problem.

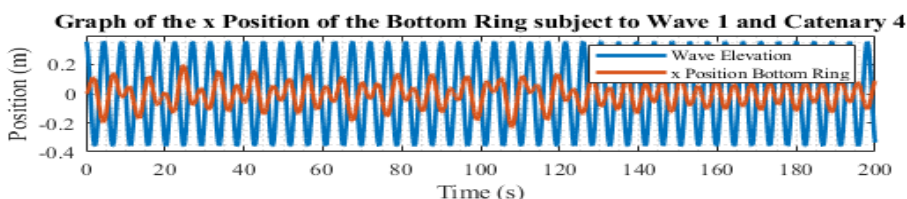


Figure 5. Comparison between wave 1 elevation and the X position of the bottom ring, considering catenary 4

With respect to the horizontal movement, all simulations showed small displacements of the structure. For the upper ring horizontal displacements, it is possible to notice that the greatest movement occurred for the wave with the shortest period. In addition, catenaries 3 and 4 proved to be more stable for this situation (Fig. 6).

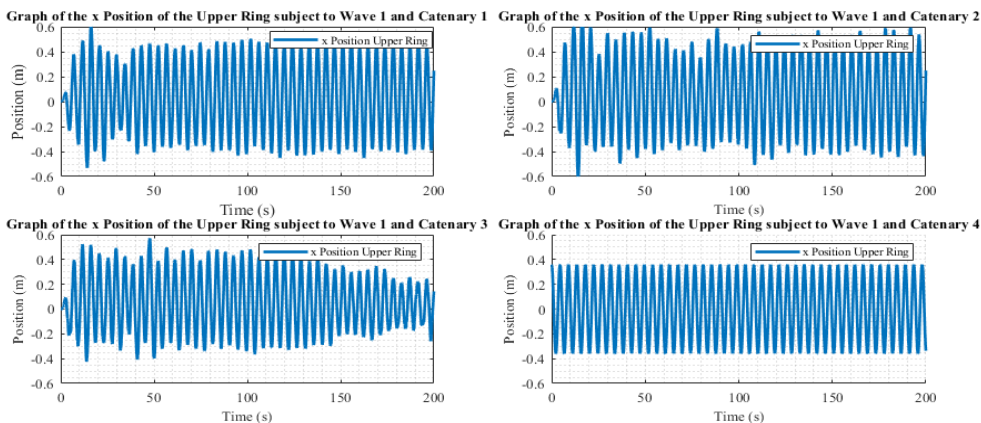


Figure 6. Position X of the upper ring for all 4 catenaries

For all waves and catenary geometries, the Y-rotation of the upper ring (R_y), as well as the Y-rotation of the lower ring, corresponded to the wave slope angle suggesting that the structure is stable (Fig. 7).

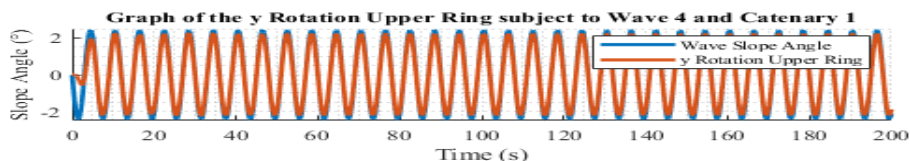


Figure 7. Comparison between wave 4 slope angle and rotation Y of the upper ring, considering catenary 1

5 Conclusion

After all tests with catenaries, it was not possible to identify a behavior pattern between the parameters, for example, that heavier materials showed more stability for the structure. Therefore, it is necessary that the definition and the validation of the mooring system occur with the hydrodynamics studies of the structure. Regarding to the cage's ring structure, the results indicate that for the study site chosen, a circular floating net cage with a smaller diameter would be more indicated, since it would decrease the column water pressure.

Finally, by applying the drag coefficient formula, the modeling of the drag force acting on the net with the software used proved to be a satisfactory solution as an approach of problems involving fish cages. However, it is important to emphasize that the used model does not consider the non-linearity of the net. Therefore, future work for this implementation is suggested.

Acknowledgements. This study was financed in part by the Coordination for the Improvement of Higher Education Personnel – Brasil (CAPES) – Finance Code 001, the National Council for Scientific and Technological Development (CNPq) and Rio Grande do Sul State Research Support Foundation (FAPERGS).

Authorship statement. The authors hereby confirm that they are the sole liable persons responsible for the authorship of this work, and that all material that has been herein included as part of the present paper is either the property (and authorship) of the authors, or has the permission of the owners to be included here.

References

- [1] FAO, 2018. *The State of World Fisheries and Aquaculture 2018 - Meeting the sustainable development goals*, Rome.
- [2] Lader, P. F. & Enerhaug B. , 2005. Experimental investigation of forces and geometry of a net cage in uniform flow. *IEEE Journal of Oceanic Engineering*, vol. 30, no. 1.
- [3] Dong, S. & You, X. & Hu, F., 2020. Effects of design factors on drag forces and deformations on marine aquaculture cages: a parametric study based on numerical simulations. *Journal Marine Science and Engineering*, vol. 8, pp. 125 .
- [4] Júnior, E. M. D., 2010. *Montagem, instalação e manutenção de tanques-rede para a criação de peixes marinhos em mar aberto*. Universidade Federal Rural de Pernambuco, Relatório Final de Engenharia de Pesca.
- [5] Assis, J. S., 2013. *Sistemas de ancoragem de plataformas: manuseio de âncoras em águas profundas*. Centro de Instrução Almirante Graça Aranha (CIAGA), Trabalho de Conclusão do Curso Aperfeiçoamento para Oficiais de Náutica da Marinha Mercante (APNT).
- [6] Kim. T. H., & Yang, K. U., & Hwang, K. S., & Jang, D. J., & Hur, J. G., 2011. Automatic submerging and surfacing performances of model submersible fish cage system operated by air control. *Aquacultural Engineering Journal*, vol. 45, pp. 74-86.
- [7] Dean, R. G. & Dalrymple, R. A., 1991. *Water wave mechanics for engineers and scientists*, Singapore: World Scientific, vol. 2.
- [8] Faltinsen, O. M., 1990. *Sea loads on ships and offshore structures*. Cambridge University Press.
- [9] BRIDON. Bridon Oil and Gas, 2013. *Products Catalogue*. Doncasters, UK.
- [10] Wichers, J. E. W., 1993. Review of state-of-the-art on experimental techniques, SNAME OC-2 panel, *Moor-ing, Stationkeeping and Marine Terminals*, subject Analytical methods and practical guidelines for Catenary mooring systems.
- [11] Wilson, J. F., 2003. *Dynamics of offshore structures*. John Wiley & Sons, Inc.
- [12] Chakrabarti, S. K., 1987. *Hydrodynamics of offshore structures*. WIT Press, London, UK 1 First edition.
- [13] Massie, W. W., 2001. *Offshore hydromechanics*. Delft University of Technology, First edition.
- [14] ANSYS, 2016. *ANSYS AQWA Manual*. Release 16.0.
- [15] SIMCOSTA. *SiMCosta Portal*, 2020. Available: <http://www.simcosta.furg.br/home>. Access in April, 2020.